Voltage tunable terahertz emission from a ballistic nanometer InGaAs/InAlAs transistor

J. Lusakowski, W. Knap, N. Dyakonova, L. Varani, J. Mateos, T. Gonzales, Yannick Roelens, S. Bollaert, A. Cappy, K. Karpierz

Voltage tuneable terahertz emission from a ballistic nanometer InGaAs / InAlAs transistor

Cite as: J. Appl. Phys. **97**, 064307 (2005); https://doi.org/10.1063/1.1861140
Submitted: 27 September 2004 • Accepted: 21 December 2004 • Published Online: 14 March 2005

J. Lusakowski, W. Knap, N. Dyakonova, et al.

Voltage tuneable terahertz emission from a ballistic nanometer InGaAs/InAlAs transistor

J. Lusakowski[a)]
GES CNRS-Université Montpellier II UMR 5650, 34095 Montpellier, France and Institute of Experimental Physics, Warsaw University, Hoża 69, 00-681 Warsaw, Poland

W. Knap and N. Dyakonova
GES CNRS-Université Montpellier II UMR 5650, 34095 Montpellier, France

L. Varani
CEM2 CNRS-Université Montpellier II UMR 5507, 34095 Montpellier, France

J. Mateos and T. Gonzalez
Universidad de Salamanca, Departamento de Fisica Aplicada, Plaza de la Merced s/n, 37008 Salamanca, Spain

Y. Roelens, S. Bollaert, and A. Cappy
IEMN-DHS UMR CNRS 8250, Avenue Poincaré, 59652 Villeneuve d'Ascq, France

K. Karpierz
Institute of Experimental Physics, Warsaw University, Hoża 69, 00-681 Warsaw, Poland

(Received 27 September 2004; accepted 21 December 2004; published online 9 March 2005)

Terahertz emission from InGaAs/InAlAs lattice-matched high electron mobility transistors was observed. The emission appears in a threshold-like manner when the applied drain-to-source voltage U_{DS} is larger than a threshold value U_{TH}. The spectrum of the emitted signal consists of two maxima. The spectral position of the lower-frequency maximum (around 1 THz) is sensitive to U_{DS} and U_{GS}, while that of the higher frequency one (around 5 THz) is not. The lower-frequency maximum is interpreted as resulting from the Dyakonov–Shur instability of the gated two-dimensional electron fluid, while the higher frequency is supposed to result from current-driven plasma instability in the ungated part of the channel. The experimental results are confirmed by and discussed within Monte Carlo calculations of the high-frequency current noise spectra. © *2005 American Institute of Physics*. [DOI: 10.1063/1.1861140]

I. INTRODUCTION

One of the main goals of modern microelectronics is the development of devices with extremely high operation frequency. To this aim, smaller and smaller transistors are fabricated to reduce the gate capacitance and carrier transit time. However, hot carrier and contact parasitic effects limit the operation frequency of up-to-date transistors to a few hundreds of gigahertz. The reason to push this limit over the terahertz (THz) domain is not only related to the desirability of increasing the speed of devices, but also to develop sources of THz radiation. The electromagnetic radiation in the THz band (corresponding to the wavelength of the order of 0.1 mm or to the quantum energy of a few meV) is useful for different kinds of nondestructive imaging[1] and medical or technical diagnostics[2]—the emerging so-called T—ray imaging.

The most interesting, from the applications point of view, seem to be THz sources based on solid state devices that offer better possibilities of integration with other optoelectronic devices within a single chip. At present, there exist a few methods of generating THz radiation from solids; some of them are based on plasma excitations by femtosecond laser pulses in low-dimensional[3] and bulk[4] semiconductors or superconductors,[5] while other ones rely on mixing laser beams with close frequencies.[6] These methods require advanced experimental equipment and their performance depends on a strong optical excitation of an appropriate semiconductor structure. It is worth noting that all these sources generate THz radiation through plasma excitations in semiconductors. On the other hand, THz radiation can also be generated by semiconductor p-Ge (Ref. 7) and quantum cascade[8] lasers.

An alternative mechanism of plasma excitation in field-effect transistors (FETs) was proposed about ten years ago by Dyakonov and Shur[9] on the basis of an exact formal analogy between the equations of the electron transport in a gated two-dimensional (2D) transistor channel and those of shallow water, or acoustic waves in music instruments. As a consequence, in analogy with the air or water flow, hydrodynamic-like phenomena should exist also in the flow of carriers in the channel. In particular, instability of this flow in the form of plasma waves was predicted to develop under particular boundary conditions. The frequency of these waves depends on the concentration of the electron fluid and the length of the transistor gate, and it can reach the THz domain if the electron concentration is sufficiently high (at least of the order of 10^{12} cm^{-2}) and the gate length is sufficiently short (in the nanometer range). The physical mecha-

a)Electronic mail: jerzy.lusakowski@ges.univ-montp2.fr

nism supporting the development of stable oscillations is the reflection of plasma waves on the borders of the transistor with subsequent amplification of the wave's amplitude. Important factors for development of such instability are an asymmetry of the drain and source sides of the transistor channel and fulfillment of appropriate boundary conditions imposed on the resonant transistor cavity. As an example, simple formulas describing the plasma oscillations can be obtained for the limiting case of a vanishing gate-to-source impedance and an infinite gate-to-drain impedance, providing an oscillation frequency $f=(eU/m)^{1/2}/4L_G$, where U is the voltage swing, e and m are the electron charge and effective mass, respectively, and L_G is the gate length.

There are a few important practical aspects of the Dyakonov–Shur theory of plasma excitations in FETs. First, this excitation can be used for the emission as well as for the detection of the electromagnetic radiation. Depending on the parameters of the transistor, both the emission and detection can be resonant (i.e., spectrally narrow) or nonresonant (i.e., spectrally broad), and the spectral characteristic of the device can be tuned by the applied drain-to-source or gate-to-source voltages. Second, the device operation is not limited to low temperatures. In that respect, the THz-emitting FET shows the advantage of the abovementioned THz lasers that are also supposed to work up to room temperature. Last but not least, this kind of resonator based on the state-of-the-art transistor offers the most promising perspectives for large-scale integration and applications.

The idea put forward by Dyakonov and Shur found recently an experimental confirmation in measurements performed on GaAs and InGaAs high electron mobility transistors (HEMTs) and Si metal-oxide-semiconductor field-effect transistors (MOSFETs). In particular, resonant[10,11] detection of THz radiation was shown in the case of GaAs HEMTs while a voltage tuneable THz emission was observed from InGaAs HEMTs.[12] Moreover, the resonant THz detection by Si MOSFETs at room temperature[13] represents a result particularly important in view of a possible integration of THz transistors in silicon-based circuits and systems.

The present article follows our recent communication of the observation of voltage-tuneable THz emission from InGaAs HEMTs.[12] The aim of the article is to give a more complete description and analysis of the observed phenomenon. In particular, we compare the experimental data with high-frequency noise spectra obtained by Monte Carlo (MC) simulations. A qualitative agreement of measured and simulated spectra allows presenting a deeper interpretation and understanding of the observed emission. The article is organized as follows. Section II describes the experimental system and the samples used; the main characteristics of the MC simulator are described in Sec. III. The experimental results are presented in Sec. IV and are discussed in Sec. V, while the main conclusions are given in Sec. VI.

II. EXPERIMENT AND DATA ANALYSIS

A lattice-matched InGaAs/InAlAs HEMT on InP substrate grown by molecular-beam epitaxy was used in this study (Fig. 1). The active layers consisted of a

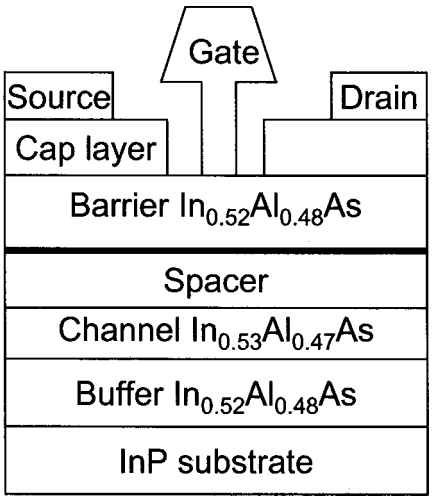

FIG. 1. Schematic structure of the transistor investigated. A structure with a T-shaped gate was used. The thick line in the barrier region shows the position of δ doping.

200 nm $In_{0.52}Al_{0.48}As$ buffer, a 20 nm $In_{0.53}Ga_{0.47}As$ channel, a 5-nm-thick undoped $In_{0.52}Al_{0.48}As$ spacer, a silicon planar doping layer of 5×10^{12} cm^{-2}, a 12-nm-thick $In_{0.52}Al_{0.48}As$ barrier layer, and, finally, a 10 nm silicon-doped $In_{0.53}Ga_{0.47}As$ cap layer with $N_D=6\times10^{18}$ cm^{-3}. The details of the technological process are given elsewhere.[14] The nominal gate length was $L_G=60$ nm, the source-drain space was $L_A=1.3$ μm, and the width of the gate was $W=50$ μm. The investigated transistor has a relatively long recess of 100 nm at both sides of the gate (the recess is the part of the channel that is not covered by the heavily doped cap layer, which improves the electrical contact of the drain and source with the channel).

All measurements were carried out at 4.2 K with the transistor placed in a liquid helium cryostat. Two Keithley 2400 source meters were used for the application of the drain-to-source (U_{DS}) and gate-to-source (U_{GS}) voltages and measurement of the drain and gate currents. The transistor was placed in a cyclotron emission spectrometer[15] designed to perform a spectral analysis of a weak THz radiation. The spectrometer consisted of two superconducting coils located one above the other and independently power supplied. The THz source and the detector were placed into both ends of a 22-cm—long copper waveguide placed in such a way that each device was in the center of an appropriate coil. Both the source and the detector of the THz radiation were cooled by a helium exchange gas to 4.2 K and totally isolated from the 300 K background radiation.

To satisfy the boundary conditions required for the plasma emission, the gate was short-circuited with the source by the shortest possible gold wire directly on the transistor chip (that decreased the gate-to-source impedance) and the transistor was driven into saturation by a sufficiently large U_{DS} (which increased the gate-to-drain impedance). The short-circuiting was done after preliminary electrical characterization of the transistor.

III. MONTE CARLO MODEL

Strictly speaking, the Dyakonov–Shur theory[10] is valid for a small electric field that corresponds to the linear part of

the output characteristic. Unfortunately, the THz emission is observed only when the transistor is driven to the saturation by a sufficiently high drain bias (due to the necessity of fulfilling the boundary conditions for the emission, as was discussed in Ref. 12). However, for transistors with ultrashort dimensions, macroscopic simulators as well as analytical models are not appropriate to describe details of the electron transport. The problem is even more complicated in the case of saturation, when large electric fields are expected to cause highly nonequilibrium conductivity conditions.

That is why, to have a better physical insight into the microscopic carrier dynamics in the transistor investigated, we performed MC simulations, which is the most adequate tool to describe the transport in ultrashort devices. As a matter of fact, due to the nanometric gate length, very high electric fields appear locally and lead to the presence of hot carrier phenomena and ballistic transport. It is well known that such phenomena can be accurately modeled in electronic devices using an Ensemble MC model self-consistently coupled to a Poisson solver.[16,17] For the special case of heterostructure devices, the physical scenario becomes particularly complex due to the appearance of quantum effects associated with energy quantization in the transversal dimension within the channel, degeneracy due to the high carrier concentration and tunneling from the channel into the gate due to the very thin barrier layer. In our simulations, degeneracy effects are locally taken into account using the rejection technique,[18] while other quantum effects have been neglected in order to have reasonable CPU times, since a dynamic self-consistent solution of Poisson and Schrödinger equations represents a formidable task even for up-to-date computers. However, being the plasma oscillations a collective motion arising from Coulomb interaction among carriers, the main features of this phenomenon are taken into account correctly in this semiclassical MC model. The microscopic simulator has been already validated through comparison with experimental results performed on similar devices and concerning static characteristics, small-signal parameters, and noise performances.[19,20]

In order to detect and emphasize the presence of plasma oscillations, special attention is devoted to the calculation of noise spectra due to their extreme sensitivity to microscopic features of carrier dynamics[21–23] and the possibility to perform a frequency analysis of electrical fluctuations.[24] For instance, the appearance of a peak in the frequency noise spectrum is a signature that the system is "ready" to develop macroscopic oscillations at that frequency if appropriate boundary conditions are fulfilled. Indeed, some features of the noise spectra presented further on are caused by macroscopic plasma oscillations in the transistor channel. To exclude from the noise spectra the contribution of numerical noise associated with the intrinsic stochastic nature of the MC method an accurate algorithm based of the Ramo–Shockley theorem[25] and its specific formulation for the case of transistors[26] has been employed for the computation of the instantaneous currents. Such an algorithm has already provided good results for the case of metal-oxide-semiconductor field-effect transistors[27] and HEMTs.[20]

In this context, it is important to emphasize that the capability of noise spectra to give precise indications on the onset of collective phenomena due to interparticle correlations has already been pointed out.[24,28–30] In particular, the presence of concentration gradients, such as those present near homo- or heterojunctions, has been found to couple the fluctuations of velocity with the fluctuations of the self-consistent electric field, which is evidenced as a peak in the noise spectra at the plasma frequency of the electronic gas.[28–33] As a consequence, the calculation of gate and drain current noise spectra of the HEMTs investigated in this work will be used to complement the experiments and to confirm the appearance of a deterministic component in the carrier dynamics associated with plasma oscillations.

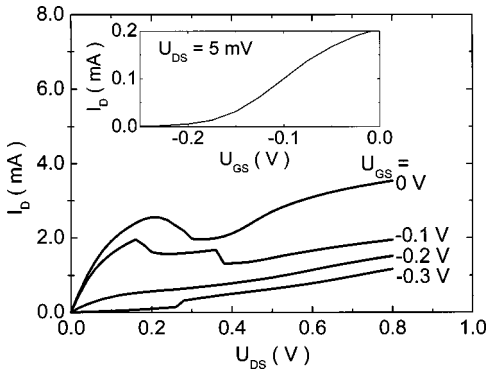

FIG. 2. Output characteristics at $T=4.2$ K, $B=0$ T of the transistor investigated at the indicated U_{GS}. The inset shows the transfer characteristic at $U_{DS}=5$ mV.

IV. RESULTS

Figure 2 shows the output and transfer (in the inset) characteristics of the transistor before the gate-source short circuit was realized. The linear part of the output characteristics is limited to U_{DS} smaller than about 20 mV. The saturation U_{DS} voltage is equal to about 0.2 V for $U_{GS}=0$ and decreases with decreasing of the gate bias.

The measurements in the magnetic field B were done with the magnetic field perpendicular to the plane of the transistor channel. Since $L_A, L_G \ll W$, the Hall voltage is short-circuited by the long drain and source metallic-like regions and the magnetoresistance of the degenerate gas appears.[34] This is the so-called geometric magnetoresistance, and the $L_A, L_G \ll W$ condition makes the investigated system analogous to that of the Corbino geometry. A significant benefit resulting from the application of the quantizing magnetic field in the present experiment was a precise determination of the electron concentration by measurements of the Shubnikov–de Haas (SdH) oscillations. The results are shown in Fig. 3 for three values of U_{GS}.

The positions of the maxima of the oscillations (shown in the inset in Fig. 3) allow determination of the electron concentration, which is equal to 2.5×10^{12} cm^{-2}. It should be noted that the positions of the maxima and minima do not depend on U_{GS}; that is, on the concentration of electrons in the gated part of the transistor. This will be discussed subsequently in connection with the electron ballistic motion under the gate.

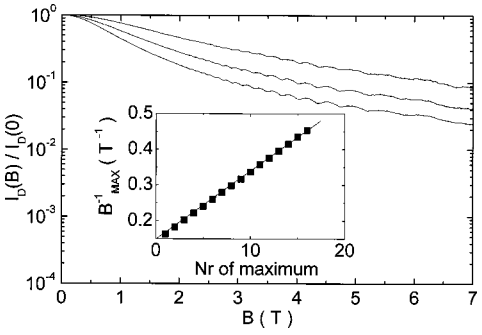

FIG. 3. SdH oscillations of the drain current $I_D(B)$ at $U_{DS}=5$ mV for three values of the gate-to-source voltage: $U_{GS}=0,-0.1$, and -0.15 V (from bottom to top). The inset shows the positions (in the inverse of the magnetic field) of the maxima of the transistor resistance.

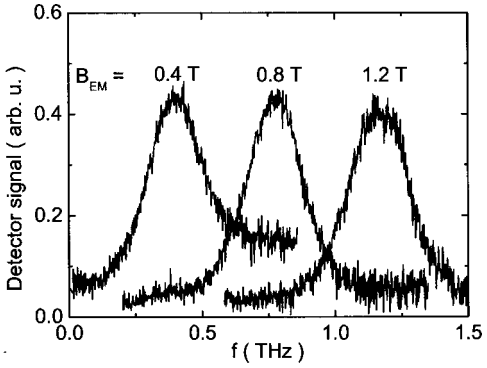

FIG. 4. Emission of the InSb epitaxial layer monitored by the InSb detector. The spectra correspond to the emitter magnetic field B_{EM} equal to 0.4, 0.8, and 1.2 T. The horizontal frequency scale is proportional to the InSb detector magnetic field.

The THz emission was analyzed by a magnetically tuneable InSb cyclotron resonance detector, biased by a dc voltage. The photoresponse signal of the detector originates from the absorption of photons with the energy $E=hf$ equal to the cyclotron resonance energy $E=heB/2\pi m$ in the InSb bulk layer (h is Planck's constant and f is the photon frequency). The absorption process causes a change of the detector resistance that is monitored by a standard lock-in technique. The reference frequency is the frequency of the U_{DS} voltage pulses applied to the transistor (or to another emitter) that emits the THz radiation as a response to the voltage pulses. In order to perform spectroscopic measurements, the InSb detector has to be calibrated; that is one must know a relation between the detector magnetic field and the frequency of photons that cause the detector photoresponse at this field. To calibrate the detector, the cyclotron emission from a bulk InSb crystal was analyzed by the InSb detector. To this aim, an epitaxial layer of InSb was placed in the magnetic field of one of the spectrometer coils and voltage pulses were applied to the layer causing a smearing of electrons over the Landau levels of the conduction band. The relaxation of electrons to the ground state occurs partially by a radiative process that is the inverse of the cyclotron resonance absorption transition. This so-called Landau emission from the same InSb crystal was previously examined by means of the Fourier transform spectroscopy.[15] Thus, the dependence of the frequency of emitted photons on the InSb emitter magnetic field is known. Some of the calibration spectra are shown in Fig. 4. Each of them corresponds to a given value of the InSb emitter magnetic field (and thus to emitted photons of a well determined energy) and was measured as a function of the InSb detector magnetic field. Since the energy of emitted photons is known, the detector magnetic field corresponding to the maximum of a curve can be converted into the frequency scale by equating $f=eB/2\pi m$. The frequency scale thus determined is the horizontal axis in Fig. 4. The output power of the InSb source used for calibration is in the picowatt range, and the emission frequency can be tuned by the magnetic field in a wide interval from a fraction of THz up to a few THz. More details on the calibration procedure and the Landau emission spectrometer can be found in Ref. 15. After the calibration procedure was completed, the bulk InSb emitter was replaced by the HEMT.

Figure 5 shows the HEMT emission spectra for different U_{DS} when the gate was short circuited with the source by the gold wire directly on the transistor chip. Each spectrum exhibits two peaks. The position of the low-frequency (LF) peak moves to higher frequencies with the increase of U_{DS}, while the position of the high-frequency (HF) peak does not change. The amplitude of the HF peak is much smaller than that of the LF one, and it appears rather as a kink in the frequency dependence of the detector signal.

To investigate the influence of the gate bias on the emission, the gold wire shorting the source and the gate was removed. The shape of the spectra so obtained changes essentially in comparison with those presented in Fig. 5: the amplitude of the LF peak considerably decreases, and the HF peak is more evident. It is remarkable that the emission spectrum is modified even when $U_{GS}=0.0$ V, indicating the importance of the transistor's boundary conditions for the emission spectra. By removing the gold wire from the chip, we replaced a loop of an extremely small conductance and capacitance with another one composed of about 3 m of screened cables that connected the source and the gate with measurement instruments outside the cryostat. The application of the gate bias (open circles in Fig. 6) decreases the amplitude of both the HF and LF peaks and also influences their relative amplitude. The spectra shown in Figs. 5 and 6

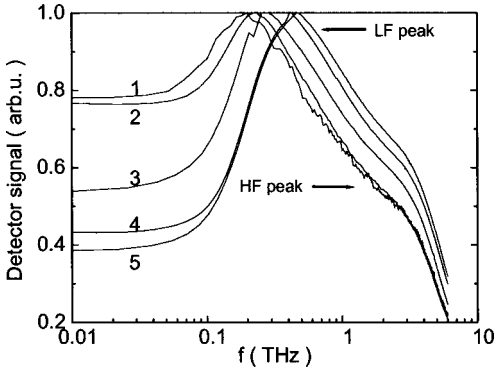

FIG. 5. InGaAs/AlInAs HEMT THz emission spectra for the gate short-circuited with the source by a gold wire on the chip. The spectra from 1 to 5 correspond to U_{DS} equal to 0.3, 0.45, 0.6, 0.7, and 0.8 V, respectively. The spectra are normalized to the maximum of the LF peak. The transistor magnetic field is equal to zero.

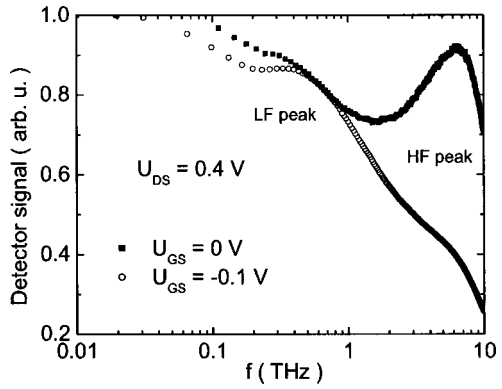

FIG. 6. Effect of the gate bias on the THz emission at $U_{DS}=0.4$ V. Solid symbols are for $U_{GS}=0$ V and open ones for $U_{GS}=-0.1$ V. The spectra are normalized at $f=0.01$ THz.

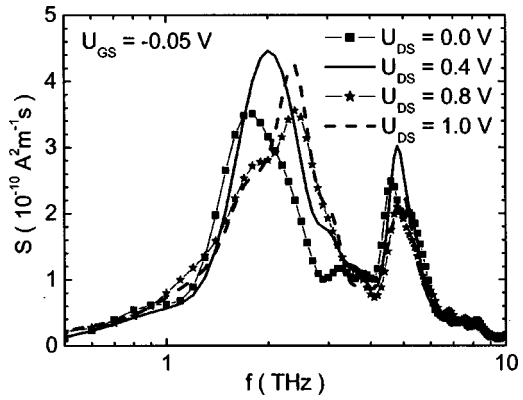

FIG. 8. Gate current noise spectra for the indicated drain-to-source voltages at a constant gate-to-source voltage of −0.05 V.

show that the position of the HF peak is not sensitive to changes in the gate or drain voltages, while the LF peak moves when the transistor bias is changed.

V. DISCUSSION

Discussion of the experimental data is based on the results of the MC simulations of electron transport in the transistor investigated. The spatial dependence of the electron velocity in the channel of the HEMT is shown in Fig. 7 for several values of the drain-source bias at a constant gate-to-source voltage of −0.05 V. These biasing conditions correspond to the saturation region of the output characteristics shown in Fig. 2. One can notice that the electrons move under the gate with a velocity of at least an order of magnitude higher than in the recess or contact parts of the transistor. This velocity increases with the drain bias and clearly shows that the ballistic regime is achieved under the gate. In view of this result, one can understand the SdH data shown in Fig. 3 that indicate that the electron concentration determined by the SdH oscillations does not depend on the gate bias. Thinking of the gated part as a flat capacitor with a gate voltage controlled electron concentration one could expect that for a strongly negative gate voltage the SdH oscillations should exhibit the influence of two different concentrations:

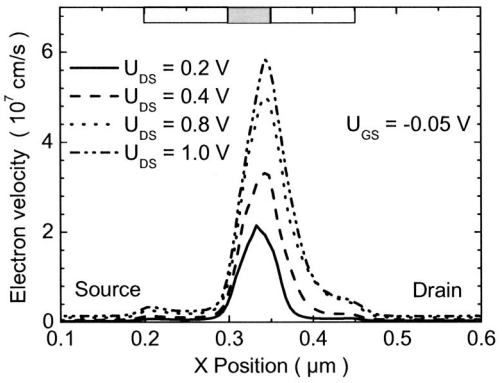

FIG. 7. Electron velocity profile in the channel of the transistor investigated for a constant U_{GS} of −0.05 V and the indicated values of U_{DS}. The dashed and clear bars at the top of the figure indicate the spatial extension of the gate and recess regions, respectively.

one corresponding to the gated part and the other one to the ungated one. In fact, for a large gate voltage (e.g., −0.1 or −0.15 V, see Fig. 3) the gated part of the transistor dominates in the total source-drain resistance and the properties of the gated part should become evident in measurements of the total source-drain magnetoresistance. However, one observes only one period of oscillations in the SdH data. To explain this fact, let us recall that the SdH oscillations result from the oscillatory character of the effectiveness of the *diffusive* electron scattering when the Fermi surface crosses subsequent Landau levels. No such scattering occurs in the ballistic regime and that explains why the SdH oscillations are not sensitive to the gate bias. It follows that the concentration determined from SdH measurements is that of the ungated part of the transistor.

The velocity distribution shown in Fig. 7 allows putting the interpretation of the observed emission spectra on a more quantitative base. Apparently, the source-drain distance breaks into two parts: the gated one, where the velocity changes significantly with the drain-to-source voltage, and the ungated one, where this influence is much weaker. We indicate a similarity of this behavior with an influence of U_{DS} on the emission spectra where the LF peak moves with U_{DS} while the HF one does not. This provides an argument for the interpretation of the LF peak as resulting from the plasma oscillations below the gate and the HF one from oscillations in the ungated part. This reasoning is further supported by an analysis of the noise spectra.

Figure 8 shows the gate current noise spectra for several values of the drain-to-source bias and a constant gate-to-source voltage. There are two maxima on each spectrum: the LF one around 2 THz and the HF one at 5 THz. The position of the HF maximum does not depend on the drain voltage, while the LF maximum moves to higher frequencies when the drain voltage increases. This is exactly what is observed in the experimental spectra shown in Fig. 4. On the other hand, there are also some discrepancies. First, in the experiment, the ratio of the amplitude of the LF to the HF peak is much larger than that found in the simulations. This, however, could be attributed to the peculiar boundary conditions imposed on the resonating transistor cavity in the experiment. The boundary conditions assumed in the simulations are closer to those corresponding to the upper curve in Fig. 6

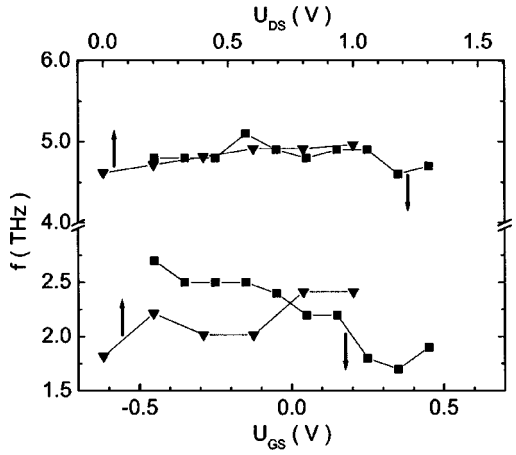

FIG. 9. Gate-to-source (bottom axis, squares) and drain-to-source (top axis, triangles) dependence of the LF and HF peaks frequency position in saturation conditions.

(solid symbols), which was registered without the short-circuiting wire. As one can see, in this case the ratio of the amplitude of LF and HF peaks is comparable to that given by the MC simulations. Second, the experimentally observed frequency of the LF peak (Figs. 5 and 6) is smaller than given by simulations (Fig. 8), while the positions of the HF peaks coincide. The difference in the frequency of the LF peak may come from the fact that the real length of the gate is larger than the nominal one assumed in the simulations (see the appropriate discussion in Ref. 12). On the other hand, the length of the ungated part is determined with a relatively higher precision, which results in the agreement of the experimental data and the MC simulations.

Figure 9 shows the frequency of the HF and LF peaks as a function of the gate-to-source voltage (bottom axis, squares) and drain-to-source voltage (upper axis, triangles). The position of the HF peak around 5 THz does not depend on the bias of the transistor. In contrast, the frequency of the LF peak increases when the transistor is drawn more and more into saturation. To explain it in more detail, let us recall that the saturation is achieved by making U_{DS} more positive at a constant gate voltage; that is, moving to the right along the top axis: the frequency marked by open triangles increases from about 2 to 2.5 THz. Such an increase is experimentally observed in Fig. 5. On the other hand, when the drain-to-source voltage is constant, the saturation is achieved by making the gate potential more negative; that is moving along the bottom axis to the left. A similar increase of the plasma frequency is then observed (squares), which corresponds to the shift of the LF peak position in Fig. 6. It should be underlined that the so far observed emission occurs only in saturation when the boundary conditions imposed on the transistor cavity are fulfilled. For the range of the drain and gate voltages in Fig. 9, the transistor is saturated.

The interpretation of the LF peak as coming from the Dyakonov–Shur instability of the *gated* 2D plasma was justified in Ref. 12 on the base of the dependence of the emission frequency on U_{DS} and the threshold-like increase of the emission signal with an increase of U_{DS}. It is further supported by the MC simulations described earlier. However, the interpretation of the origin of the HF peak is not so evident. In the experiment, the emission at the LF and HF peaks always appears at the same threshold voltage. Thus, the HF peak could correspond to a broad spectrum of oblique modes under the gate; that is, to plasma excitations propagating with a nonzero component of the wave vector along the longer dimension of the gate. On the other hand, one cannot exclude oscillations in the ungated part. In such a case, however, a question arises: are these oscillations caused by the flow of the current (current-driven instability similar to that described by the Dyakonov–Shur theory[9]) or by a coupling to the oscillating gated plasma? To the best of our knowledge, no theory exists at the moment that shows that a current flow could lead to instability of an ungated electrongas. Interpretation of the HF peak requires further experimental and theoretical investigation.

VI. CONCLUSIONS

Terahertz emission due to plasma instability in InGaAs/InAlAs HEMT was observed as a function of the drain-to-source and gate-to-source voltages. The emission was observed in the saturation of the transistor and its spectrum consists of two peaks with frequencies around 5 THz and around 1 THz. The HF peak does not move when the gate-to-source or drain-to-source voltages change. The position of the LF peak depends on the transistor bias. HF noise spectra obtained by the MC simulations also showed two peaks whose frequency and bias dependencies agree with those observed experimentally. MC simulations confirm the interpretation of the LF peak as resulting from the Dyakonov–Shur plasma instability in the gated part of the transistor. Possible origin of the HF peak is discussed. MC simulations showed also that the electron motion under the gate is ballistic. This is in agreement with the fact that the Shubnikov–de Haas oscillations do not depend on the gate bias.

ACKNOWLEDGMENTS

The authors are thankful to M. Dyakonov, M. Shur, M. Levenstein, and V. Popov for stimulating discussions. This work has been partially supported by the Dirección General de Investigación (Ministerio de Ciencia y Tecnología) and FEDER through the project TEC2004-05231.

[1] E. B. Cole, R. Woodward, D. A. Crawley, V. P. Wallace, and D. Arnone, Proc. SPIE **4276**, 1 (2001).
[2] B. H. Deng, C. W. Domier, A. J. Donne, K. C. Lee, N. C. Luhmann Jr., E. Mazzucato, T. Munsat, H. Park, and M. van-de-Pol, IEEE MTT-S Int. Microwave Symp. Dig. **3**, 1587 (2002).
[3] N. Sekine, K. Hirakawa, M. Vosseburger, P. H. Bolivar, and H. Kurz, Phys. Rev. B **64**, 201323/1-4 (2001); R. Bratschitsch, R. Kersting, T. Muller, G. Strasser, K. Unterrainer, W. Fischler, and R. A. Hopfel, Physica B **272**, 375 (1999).
[4] J. N. Heyman, P. Neocleous, D. Hebert, P. A. Crowell, T. Muller, and K. Unterrainer, Phys. Rev. B **64**, 085202/1-7 (2001); D. Hashimshony, A. Zigler, and K. Papadopoulos, Phys. Rev. Lett. **86**, 2806 (2001); T. Dekorsy, H. Auer, H. J. Bakker, H. G. Roskos, and H. Kurz, Phys. Rev. B **53**, 4005 (1996).
[5] I. Iguchi, Semicond. Sci. Technol. **13**, 93 (2000).
[6] S. Hoffmann, M. Hofmann, E. Brundermann, M. Havenith, M. Matus, J. V. Moloney, A. S. Moskalenko, M. Kira, S. W. Koch, S. Saito, and K. Sakai, Appl. Phys. Lett. **84**, 3585 (2004).

[7]A. A. Andronov, V. A. Kozlov, S. A. Pavlov, and S. G. Pavlov, Sov. Tech. Phys. Lett. **14**, 891 (1988).
[8]R. Kohler, A. Tredicucci, C. Mauro, F. Beltram, H. E. Beere, E. H. Linfield, A. G. Davies, and D. A. Ritchie, Appl. Phys. Lett. **84**, 1266 (2004).
[9]M. Dyakonov and M. S. Shur, Phys. Rev. Lett. **71**, 2465 (1993); M. Dyakonov and M. S. Shur, in *Terahertz Sources and Systems*, edited by R. E. Miles (Kluwer Academic, Dordrecht, 2001), p. 187.
[10]W. Knap, Y. Deng, S. Rumyantsev, J.-Q. Lü, M. S. Shur, C. A. Salor, and L. C. Brunel, Appl. Phys. Lett. **80**, 3433 (2002); W. Knap, Y. Deng, S. Rumyantsev, and M. S. Shur, *ibid.* **81**, 4637 (2002).
[11]X. G. Peralta, S. J. Allen, M. C. Wanke, N. E. Harff, J. A. Simmons, M. P. Lilly, J. L. Reno, P. J. Burke, and J. P. Eisenstein, Appl. Phys. Lett. **81**, 1627 (2002).
[12]W. Knap, J. Łusakowski, T. Parenty, S. Bollaert, A. Cappy, V. V. Popov, and M. S. Shur, Appl. Phys. Lett. **84**, 2331 (2004).
[13]W. Knap, F. Teppe, Y. M. Meziani, N. Dyakonova, J. Łusakowski, F. Boeuf, T. Skotnicki, D. Maude, S. Rumyantsev, and M. S. Shur, Appl. Phys. Lett. **85**, 675 (2004).
[14]T. Parenty, S. Bollaert, J. Mateos, X. Wallart, and A. Cappy, *Proc. of Indium Phosphide and Related Material (IPRM) Conference*, Nara, Japan, May 2001, p. 626.
[15]W. Knap, D. Dur, A. Raymond, C. Meny, J. Leotin, S. Huant, and B. Etienne, Rev. Sci. Instrum. **63**, 3293 (1992).
[16]C. Jacoboni and L. Reggiani, Rev. Mod. Phys. **55**, 645 (1983).
[17]C. Jacoboni and P. Lugli, *The Monte Carlo Method for Semiconductor Device Simulation*, (Springer, Vienna, 1989).
[18]P. Lugli and D. K. Ferry, IEEE Trans. Electron Devices **ED-32**, 2431 (1985).
[19]J. Mateos, T. González, D. Pardo, V. Hoel, and A. Cappy, Semicond. Sci. Technol. **14**, 864 (1999).
[20]J. Mateos, T. González, D. Pardo, V. Hoel, and A. Cappy, IEEE Trans. Electron Devices **47**, 1950 (2000)
[21]Sh. Kogan, *Electronic Noise and Fluctuations in Solids* (Cambridge University Press, Cambridge, UK, 1996).
[22]*Noise and Fluctuations Control in Electronic Devices*, edited by A. Balandin (American Scientific, Stevenson Ranch, CA, 2002).
[23]*Proceedings of the 17th Int. Conf. on Noise and Fluctuations Physical Systems*, edited by J. Sikula (CNRL s.r.o., Brno, Czech Republic, 2003).
[24]L. Varani, L. Reggiani, T. Kuhn, T. González, and D. Pardo, IEEE Trans. Electron Devices **41**, 1916 (1994).
[25]B. Pellegrini, Phys. Rev. B **34**, 5921 (1986).
[26]A. Kim, A. S. Min, T. W. Tang, and Y. J. Park, Solid-State Electron. **34**, 1251 (1991).
[27]T. González, D. Pardo, L. Varani, and L.Reggiani, IEEE Trans. Electron Devices **42**, 991 (1995).
[28]L. Varani and L. Reggiani, Riv. Nuovo Cimento **17**, ser. 3(7), 1 (1994).
[29]L. Varani, *Proc. of the 13th Int. Conf. on Noise in Physical Systems and* $1/f$ *Fluctuations*, edited by V. Bareikis and R. Katilius (World Scientific, Singapore, 1995) p. 209.
[30]L. Reggiani, P. Gilinelli, E. Faucker, L. Varani, T. González, and D. Pardo, *Proc. of the 13th Int. Conf. on Noise in Physical Systems and* $1/f$ *Fluctuations*, edited by V. Bareikis and R. Katilius (World Scientific, Singapore, 1995), 018 p. 163.
[31]E. Starikov, P. Shiktorov, V. Gruzhinskis, J. P. Nougier, J. C. Vaissière, L. Varani, and L. Reggiani, Appl. Phys. Lett. **66**, 2361 (1995).
[32]P. Shiktorov, V. Gruzhinskis, E. Starikov, L. Reggiani, and L. Varani, Phys. Rev. B **54**, 8821 (1996).
[33]T. González, D. Pardo, L.Reggiani, and L. Varani, J. Appl. Phys. **85**, 2349 (1997).
[34]A. C. Beer, *Galvanomagnetic Effects in Semiconductors*, in Solid State Physics, Suppl. 4 (Academic, New York, 1963).